International Journal of Thermal Technologies
ISSN 2277 - 4114

Available at http://inpressco.com/category/ijcet

Research Article

Numerical Analysis of the Flow Through in Centrifugal Pumps

Mohan Lamloumi Hedi[a*], Kanfoudi Hatem[a], Zgolli Ridha[a]

[a]Ecole Nationale d'Ingénieurs de Tunis (ENIT. Laboratoire de Modélisation en Hydraulique et Environnement (LMHE).
B.P. 37. Le Belvédère, 1002 Tunis, Tunisia department, University1, city, country

Accepted8 Nov.2012, Available online 1Dec. 2012, Vol.2, No.4(Dec. 2012)

Abstract

In order to investigate the flow structure in centrifugal pump, a numerical model based on three dimensional (3D) incompressible Reynolds-Averaged Navier-Stokes equations has been developed. The turbulence viscosity is computed using the SST model (Shear Stress Transport). These transport equations associated with the appropriate boundaries conditions are solved by the CFX-13 finite-volume code. The computational domain composed by a single stator and rotor blade passages is discretized by a structured multi-block meshes. It describes in detail the numerical approach, based on an approach URANS (Unsteady Reynolds Average Navier Stokes) to predict the pressure fluctuations. On the other hand, simulations digital steady are made to construct the performance for centrifugal pump (NS32). The unsteady simulations have allowed access to the temporal behavior of internal flow and compare the influence of two parameters in particular: mesh and conditions limits finding it difficult to model the pressure fluctuation The velocity and pressure fields show a radial thrust. Conformed to experimental visualization.

Keywords*: Centrifugal pump, pressure distribution, velocity distribution, SST turbulence model*

1. Introduction

Centrifugal pumps are used in a variety of applications, such as, water supply and irrigation, power –generating utilities, flood control, sewage handling and treatment, process industries, transporting liquid-solid mixtures. Conventional design method of centrifugal pump are largely based on the application of empirical and semi-empirical rules along with the use of available information in the form of different types of charts and graphs as proposed by successful designers .As the design of centrifugal pump involve a large number of interdependent variables, several other alternative design are possible for same duty. Computational fluid dynamics (CFD) is being increasingly applied in the design of the centrifugal pumps. 3-D numerical computational fluid dynamics tool can be used for simulation of the flow field characteristics inside the turbo machinery. Numerical simulation makes it possible to visualize the flow condition inside a centrifugal pump, and provides the valuable hydraulic design information of the centrifugal pumps.

In non cavitating flow in the pump, the main difficulty is to better reproduce the complex geometry configuration of the flow domain. To overcome these difficulties, some simplifications in the geometry are often considered. In the literature, many hydrodynamic models are reported in two (2D) and three dimensional (3D) by using the CFD code. (Croba et al 1996) simulated the (2D), unsteady water flow in centrifugal pump. (Blanco et al.2000) simulated the (3D) fluid flow in the centrifugal pump to evaluate the pressure fluctuation in the volute. (Huang et al 2010). simulated the (3D) flow in the centrifugal pump by using the sliding meshes for analyzing the flow structure. (Shojaee Fard et al 2002) studied numerically and experimentally the performance of the centrifugal pump for different geometries of impeller.

(Shum et al 2000). And (Akhras et al 2004). studied impeller diffuser interaction on the pump
performance and showed that a strong pressure fluctuation is due to the unsteadiness of the flow shedding from impeller.

(Zhang et al1996). found that jet-wake structure occurs near the outlet of the impeller and it is independent of flow rate and locations.

(Liu et al.1994) and (Pedersen et al 2003)have made the measurement on centrifugal pumps and reported that impeller flow separation was observed on blade surface at off-design flow rate as compared to smooth flow within the impeller passage at design point.

In this study, a numerical model is used to calculate steady hydrodynamics and unsteady in NS32 pump. A structured grid was used in the impeller and unstructured grid in the volute. To evaluate the effect of turbulence model on the flow field, the k–$\varepsilon$and SST turbulence models were tested.. The unsteady simulations have allowed access to the temporal behavior of internal flow and compare the influence of two parameters in particular: mesh and conditions limits finding it difficult to model the pressure fluctuation.

*Corresponding author's Email: hedilamloumi@gmail.com

2. Mathematical formulation.

2.1 Governing equations

The flow in axial pump is considered as a steady, three dimensional and turbulent flow. The relevant governing equations are the mass conservation, the Reynolds averaged Navier-Stokes (RANS) and the appropriate turbulent viscosity closure model.

2.1.1 The Reynolds Averaged Navier-Stokes

Assuming that the fluid is incompressible, the mass conservation equation is written in tensor notation and in cartesian coordinates

$$\frac{\partial \rho}{\partial t} + \frac{\partial(\rho u_j)}{\partial x_j} = 0 \quad (1)$$

where $\rho$is the water density; Ui and x_i are respectively the average velocity components and coordinates in the direction i.

The derivation of RANS equations is based on the Reynolds decomposition applied to the instantaneous Navier-Stokes equations. For incompressible fluid, these equations are:

$$\frac{\partial(\rho u_i)}{\partial t} + \frac{\partial(\rho u_j u_i)}{\partial x_j} = -\frac{\partial p}{\partial x_i} + A + F_i \quad (2)$$

Where A is a turbulent and laminar diffusive term given by :$A = \frac{\partial}{\partial x_j}\left[(\mu_m + \mu_t)\left(\frac{\partial u_i}{\partial x_j} + \frac{\partial u_j}{\partial x_i}\right)\right]$ (3)

P: the pressure

Fi : the additional sources of momentum

Since the momentum equations are considered in a relative reference frame associated to the rotor blade, the Coriolis force and centrifugal forces are added as a momentum source term:

$F_i = F_{i,co} + F_{i,ce}$ (4)

Where:

$F_{i,co} = -2\varepsilon_{ijk}\omega_j u_k$ (5)

$F_{i,ce} = -\omega_j\omega_i x_j + \omega_j\omega_j x_i$ (6)

ω_i : is angular velocity and ε_{ijk} is Levi-Civita third order tensor

2.1 .2Turbulence model

In order to test the effect of turbulence model on the flow field structure, the standard SST (Menter, 1993, Johnston (1998) are considered. In these models, the nonlinear Reynolds stress term $-\rho\overline{u_i' u_j'}$is modeled using the Boussinesq hypothesis which assumes that the turbulent viscosity μ_t is isotropic

$$\tau_{ij} = -\rho\overline{u_i' u_j'} = \mu_t\left(\frac{\partial U_i}{\partial x_j} + \frac{\partial U_j}{\partial x_i}\right) - \frac{2}{3}\rho k\delta_{ij} \quad (7)$$

In order to accurately predict the flow separation from smooth surfaces, the eddy-viscosity formulation is given by:

$\mu_t = \rho\frac{k}{max(\omega, SF_2)}$(8)

Where S is the strain rate and F_2 is a second blending function defined by:

$$F_2 = tanh\left(\left(max\left(\frac{\sqrt{k}}{\beta\omega y}, \frac{500v}{y^2\omega}\right)\right)\right)^2 \quad (9)$$

2.1 .2.1*The Shear-Stress-Transport model*

The unknown turbulent viscosity μ_t is determined by solving two additional transport equations for the turbulence kinetic energy k, and for the turbulence frequency ω. These two transport equations can be written as:

$$\frac{\partial \rho U_j k}{\partial x_j} = \frac{\partial}{\partial x_j}\left[\left(\mu + \frac{\mu_t}{\sigma_{k3}}\right)\frac{\partial k}{\partial x_j}\right] + P_k - \beta\rho k\omega \quad (10)$$

Where:

Pk : shear production of turbulence.

F_1: is the first SST blending function

$$F_1 = tanh\left(min\left(max\left(\frac{\sqrt{k}}{\beta\omega y}, \frac{500v}{y^2\omega}, \frac{4\rho\sigma_{\omega 2}k}{CD_{k\omega}y^2}\right)\right)\right)^4 \quad (11)$$

Where y is the distance to the nearest wall.

$$CD_{k\omega} = max\left(2\rho\sigma_{\omega 2}\frac{1}{\omega}\frac{\partial k}{\partial x_j}\frac{\partial \omega}{\partial x_j}, 10^{-10}\right) \quad (12)$$

The table 1 gives the considered values of the (k-ω) turbulence model (Wilcox,2008)

Table 1 : The SST turbulence model constants

$\sigma_{\omega 2}$	$\sigma_{\omega 3}$	β_3	$\beta^{'}$	σ_{k3}	α_3
0.856	□□□	Mar-40	0.09	0.85	0.44

3.Steady flow in centrifugal pump

3.1Problem description

The purpose of this study is to predict numerically the flow structure in centrifugal pump with specific speed of 32 (Pump NS32), Figure. 1. Numerical simulations are performed for a determined relative position of the machine components, and then this relative position is changed in a quasi-unsteady calculation. The main pump parameters and geometry are presented in Table 1.

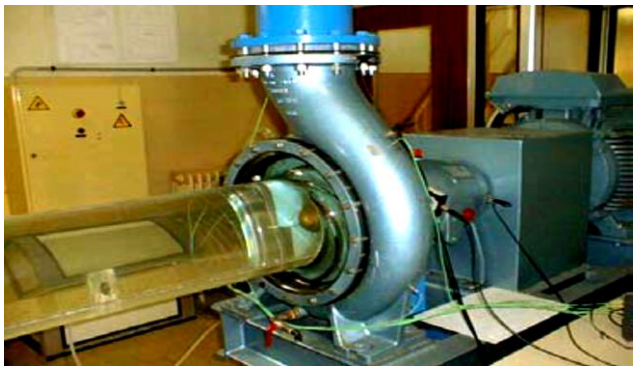

Figure 1: Experimental setup of the NS32 pump Asuaje (2005)

Table 1 : Geometrical parameters of the pump NS32.

Flow simulation domain	Impeller and volute
Grid	Impeller structured, volute unstructured
Fluid	Water at standard conditions
Inlet	Total pressure = 1 atm
Outlet	Mass flow = q (kg/s)
Turbulence model	k-ε and SST
Interface impeller-volute	Frozen rotor
Convection scheme	second order
RMS (root mean square)	4-Oct

3.2. Boundaries conditions

At the inlet of the computational domain an imposed pressure is specified (Table 2 and Fig. 2). At the outlet a mass flow q is imposed following the operating condition (Table 3). A no-slip flow condition is applied on the walls (on the blade, hub and shroud). Due to the change between the reference frame of the static volute and rotating impeller, the interaction of impeller-volute has been simulated using the Frozen-Rotor interface model (Table 2).

Table 2 : Boundaries conditions of the pump NS32.

Parameters	Value	Description
Impeller		
R_i	115 mm	Inlet flange radius
R_1	75 mm	Mean impeller inlet radius
b_1	85.9 mm	Inlet impeller width
β_1	70°	Inlet blade angle
θ_1	37°	Blade LE inclination angle
R_2	204.2 mm	Mean impeller outlet radius
b_2	42 mm	Outlet impeller width
β_2	63°	Outlet blade angle
θ_2	90°	Blade TE inclination angle
Na	5	Blade number
e	8 mm	Blade thickness
Volute		
R_3	218 mm	Base volute radius
b_3	50 mm	Volute width
$\phi_{ουτλετ}$	200 mm	Outlet flange diameter

The original configuration of the outlet volute casing was modified in order to avoid the occurrence of a big recirculation in this area. The extension of the volute outlet is essential for numerical and physical reasons, since convergence problems and related flow instabilities are prevented if the swirling zone is captured into the simulation domain

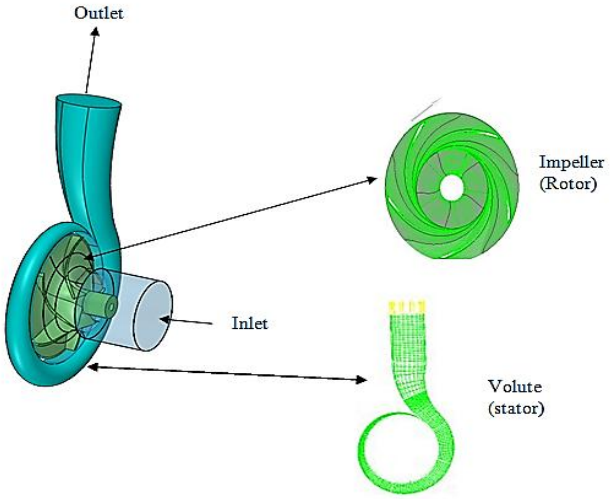

Figure 2: Grids of the isolated impeller and volute of the pump NS32.

Table 3 : Value of different mass flow

Mass flow q/q_v					
Value	0.2	0.4	0.6	0.8	1

3.3Numerical Investigation

The transport equations associated with the given boundaries conditions describing the internal flow in centrifugal pump are solved by the CFX code. This code is based on the finite-volume method to discretize the transport equations (ANSYS-CFX, 2013). For all presented numerical results, the momentum and continuity equations are solved simultaneously. In CFX, the pressure and velocity coupling is solved using the Rhie-Chow algorithm. Second order high resolution scheme have been adopted for convection terms. The source term evaluating the vaporization and condensation processes is implemented in the CFX code.

3.4Effect of turbulence on flow structure

A structured grid was used for the impeller and unstructured grid for the volute of the NS32 pump (Figure. 2). This grid is symmetric for all the five blade passage. In order to satisfy the validity of wall function treatment, a fine grid is imposed near the walls. For the nominal flow rate qv, the effect of k-ε and SST turbulence models on the pump head is presented in Figure. 3. The first turbulence model overestimates the pump head. Hence, the SST model is adopted for steady and unsteady flow. Figure. 4 shows that this model can better reproduce pump head for different mass flow.

The Figure. 5 presents the vortex behavior in pump. The vortex gives the change of the fluid particles direction that generally induces a dissipation of energy through friction.

This is due to a pressure difference between outlet of volute and inlet.

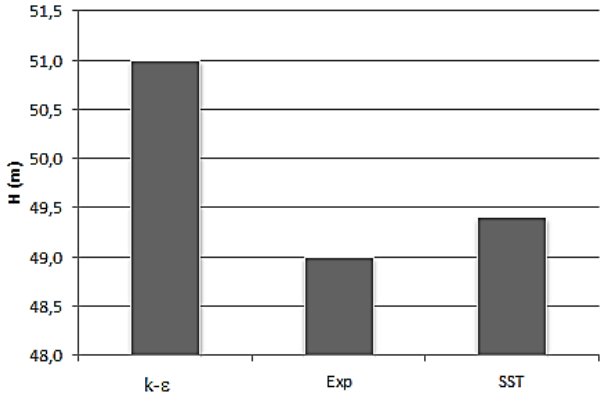

Figure 3: Influence of turbulence model on the calculated pump head.

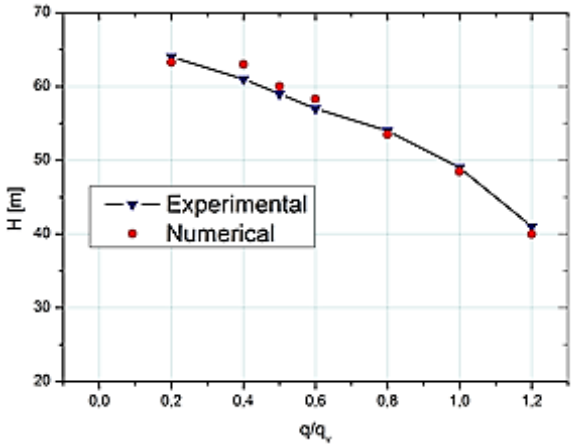

Figure 4: Comparison of experimental and numerical pump head

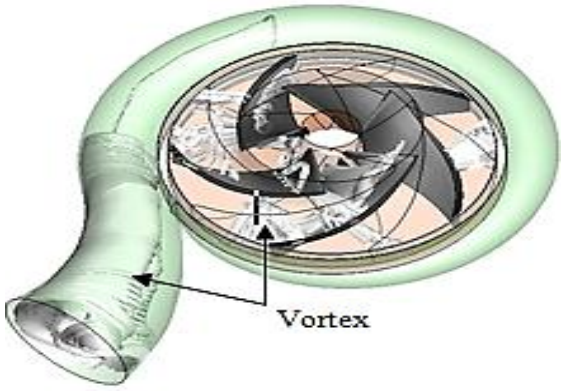

Figure 5: Numerical simulation of three dimensional vortex.

3.5 Pressure distribution and blade loading

The blade loading of pressure and suction side are drawn at three different locations on the blade at the span of 20, 50 and 80 from hub towards the shroud. The pressure loading on the impeller blade is shown in fig 6 Pressure load on the impeller blade is plot along the streamwise direction. The pressure difference on the pressure and suction sides of the blade suggests that the flow inside the impeller experiences the shearing effects due to the pressure difference on blade-to-blade passage wall.

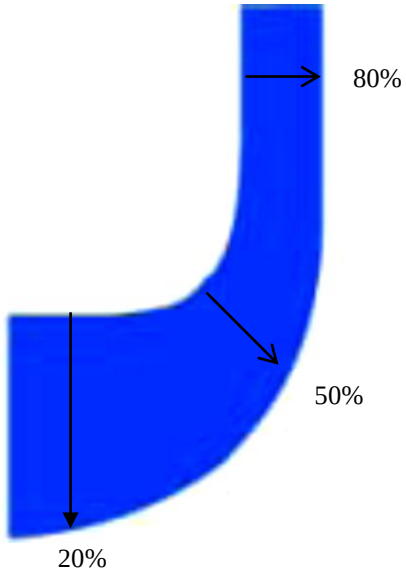

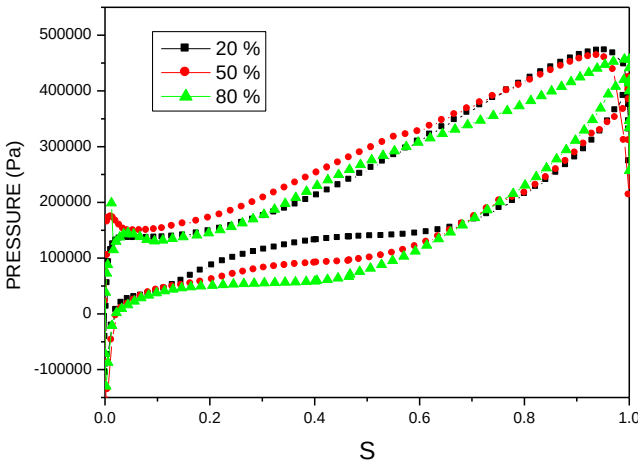

Figure 6. Blade loading at 20, 50 and 80 span

3.6 Unsteady flow

To study the behavior of pressure fluctuations in the pump NS32, cutting the middle of the length of extension is provided on the wheel and the scroll. These two sections will to study the time course of pressure fluctuations during operation of the pump. the purpose of this study is to find correlations between the behavior of fluctuations, flow and blade position relative to the spout volute. The contours representing fluctuations pressure are shown in Figure 7.

The outlines of the pressure fluctuations at t = 0.004s are in the middle of the scale of the wheel and volute, the position of the blade is a little further volute spout, but you can see a blue box (high amplitude) left by the blade (trailing edge), which is close to the spout. There is training an area of large amplitude fluctuations in the nozzle casing and another near the exit this region as the blade begins to move towards the spout (t = 0.016s). In

addition, the channel interaubage, specifically on the upper surface of the blade, there is an area where the fluctuation begins to increase slowly. For t = 0.024s, we see in the area of the nozzle, the growth of a region high amplitude close to the outlet of the spout and also the suction side of the blade. Ditto for t = 0.028 s, except that the high amplitude region increases gradually as the vane tends to approach in this area in the region of the mouth of volute.

When t = 0.032s, we note that near the nozzle volute, the high amplitude region extends from Similarly in the suction side of the blade. The alignment of the trailing edge with the spout volute manifested by the presence of a region of strong fluctuations which covers more than half of the blade and an area of the same intensity fluctuations near the spout to the inner surface of the volute. This is also accompanied by the presence of a small area of high amplitude at the trailing edge of the blade is upstream of the blade, near the beak (t = 0.036s). The region near the nozzle extends and also the source of hydraulic noise at the trailing edge remains constant. For these two moments, distance between the blade and volute spout is the smallest and the fluctuations are higher by moments or with other positions of the wheel.

Wheel slip for a few seconds (t = 0.04s) and the region of strong fluctuations begins to shrink until dawn away enough of the bill to return to the values of fluctuations lower while another approach and the same behavior of pressure fluctuations in the impeller and the volute is repeated. For all these moments, we can say that the relative position between the impeller and the volute spout does not significantly change the magnitude of fluctuations in the trailing edge of the blade which is one of the main sources of hydraulic noise. On the other hand, fluctuations in pressure in the nozzle varies according to the scroll position of the blade (they are stronger when dawn is approaching). As the distance between the tip and the trailing edge is reduced, the area of high fluctuations in the suction and grows in the region near the spout inwardly. This behavior is periodically repeated for

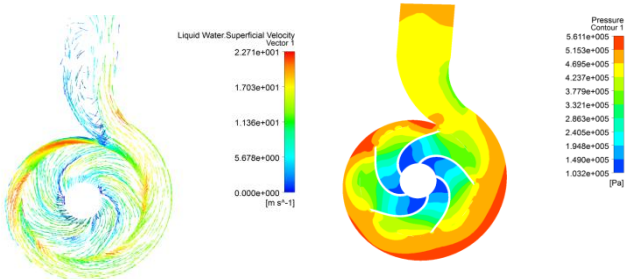

Velocity and pressure at t =0s

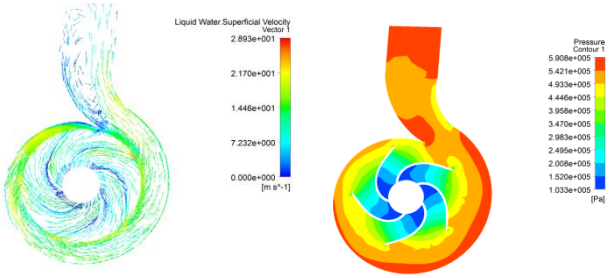

Velocity and pressure at t =0.004s

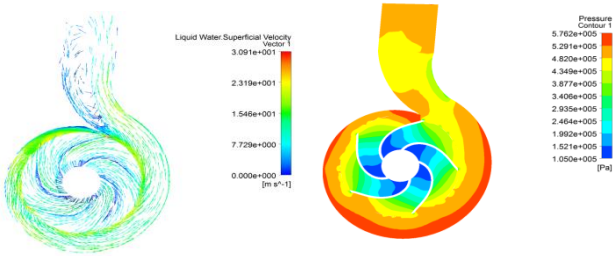

Velocity and pressure at t =0.008s

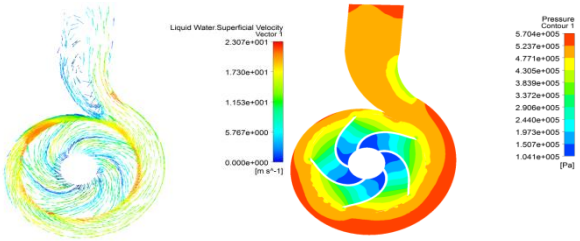

Velocity and pressure at t =0.012s

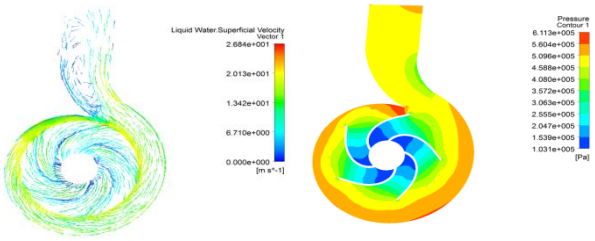

Velocity and pressure at t =0.016s

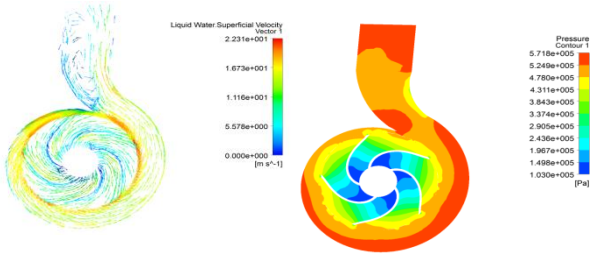

Velocity and pressure at t =0.02s

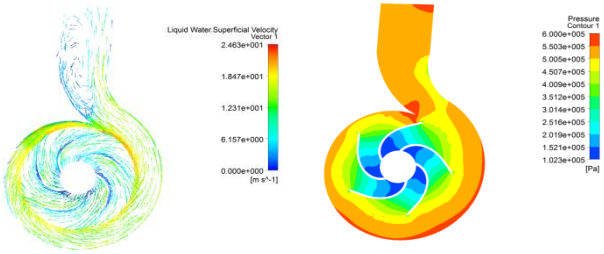

Velocity and pressure at t =0.024s

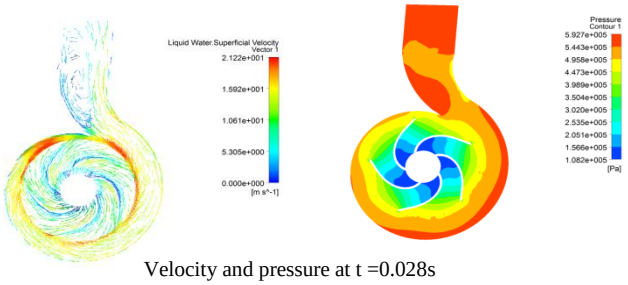

Velocity and pressure at t =0.028s

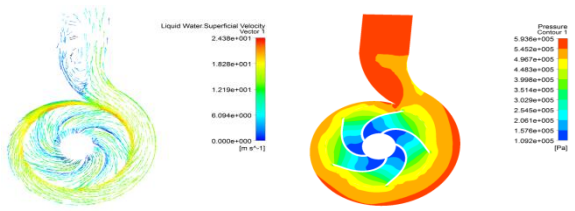

Velocity and pressure at t =0.032s

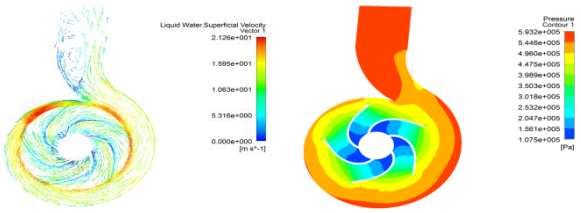

Velocity and pressure at t =0.036s

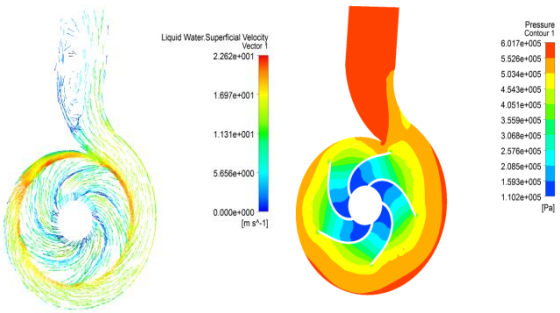

Velocity and Velocity and pressure at t =0.04s

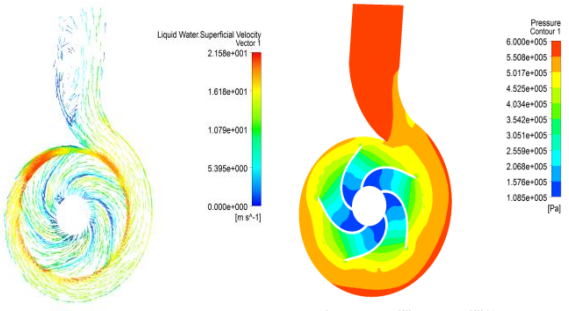

Velocity and pressure at t =0.044s

Figure 6: Contours of velocity and pressure (Pa) in the pump NS32.

Conclusion

modeling and predicting unsteady flow fluctuations pressure of two centrifugal pumps with volute were presented in all its stages. The Numerical results are provided access to the morphology of the internal flow, and confirm complexity. The interaction between the movable part constituted by the wheel and the fixed portion constituted by the volute has been demonstrated by calculating the fluctuating pressure on the wall of the volute into several strategic points and lines on the suction and discharge. On the other hand, the spectrum lines obtained from these pumps was calculated from the signals of the temporal pressure through virtual sensors. The influence of the choice of boundary conditions and the mesh is highlighted for both geometric models

References

D. Croba, and J.L. Kueny, (1996). Numerical Calculation of 2D, Unsteady Flow in Centrifugal Pumps: Impeller and Volute Interaction. *International Journal for Numerical Methods in Fluids*, Vol. 22, pp. 467-481.

E. Blanco, J. Fernández, J. González and C. Santolaria (2000). Numerical Flow Simulation in a Centrifugal Pump with Impeller-Volute Intraction. Proceedings of the ASME Fluids Engineering Division Summer Meeting.

Si. Huang , A. A. Mohamad , K. Nandakumar, Z. Y. Ruan and D. K. Sang (2010). Numerical simulation of unsteady flow in a multistage centrifugal pump using sliding mesh technique. *Progress in computational fluid dynamics*, Vol. 10, no4, pp. 239-245

M.H. Shojaee Fard, and M.B. Ehghaghi (2002). Experimental and Numerical Study of Centrifugal Pump in the Performance of Viscous Flow. *International Journal of Engineering Science*, Vol. 13, No. 3, pp. 35-52.

Wilcox, D.C. (2008). Formulation of the k-omega Turbulence Model Revisited. *Journal American Institute of Aeronautics and Astronautics*, Vol. 46, No. 11 pp. 2823-2838.

M. Asuaje, F. Bakir, S. Kouidri, F. Kenyery and R. Rey (2005). Numerical Modelization of the Flow in Centrifugal Pump: Volute Influence in Velocity and Pressure Fields. *International Journal of Rotating Machinery*, Vol 3, pp. 244-255

Menter F. et Kuntz M. Development and application of a zonal des turbulence model for cfx-5 : ANSYS-CFX Canada Ltd., CFX-Validation Report, 2002.

Johnston, J.P. (1974) The effects of rotation on boundary layers in turbomachine rotors, *Fluid Mechanics, Acoustics, and Design of Turbomachinery*,

Eds. B. Lakshminarayna, W. R. Britsch and W. S. Gearhart, pp. 207-249, NASA SP-304.Y. K. P. Shum,C. S.Tan, andN. A. Cumpsty, Impeller-diffuser interaction in a centrifugal compressor, *Journal of Turbomachinery*,
vol. 122, no. 4, pp. 777–786, 2000.

A. Akhras, M. El Hajem, J.-Y. Champagne, and R.Morel, The flow rate influence on the interaction of a radial pump impeller and the diffuser, *International Journal of Rotating Machinery*, vol. 10, no. 4, pp. 309–317, 2004.

M.-J. Zhang, M. J. Pomfret, and C. M. Wong, Performance prediction of a backswept centrifugal impeller at off-design point conditions, *International Journal for Numerical Methods in Fluids*, vol. 23, no. 9, pp. 883–895, 1996.

C. H. Liu, C. Vafidis, and J. H.Whitelaw, Flow characteristics of a centrifugal pump, *ASME Journal of Fluids Engineering*,vol. 116, no. 2, pp. 303–309, 1994.

N. Pedersen, P. S. Larsen, and C. B. Jacobsen, Flow in a centrifugal pump impeller at design and off-design conditions—part I: particle image velocimetry (PIV) and laser Doppler velocimetry (LDV) measurements, ASME Journal of Fluids Engineering, vol. 125, no. 1, pp. 61–72, 2003.